PHYSICAL REVIEW C **81**, 034613 (2010)

α decay of even-even superheavy elements

V. Yu. Denisov and A. A. Khudenko
Institute for Nuclear Research, Prospect Nauki 47, 03680 Kiev, Ukraine
(Received 12 February 2010; published 31 March 2010)

The α-decay half-lives of even-even superheavy elements within the range of proton number $104 \leqslant Z \leqslant 126$, which can be formed by possible cold and hot fusion reactions, are calculated in the framework of various approaches for α-decay half-life evaluation and by using the Q values of α transitions obtained within different approximations for atomic masses. The dependencies of α-decay half-lives of superheavy elements on model approaches for both the Q values and half-life calculations are discussed in detail.

DOI: 10.1103/PhysRevC.81.034613 PACS number(s): 23.60.+e, 21.10.Tg, 24.10.−i, 27.90.+b

I. INTRODUCTION

The synthesis of superheavy elements (SHEs) is a very interesting problem and hot topic in nuclear physics. The question "Where is the border of the elements' existence?" still has no answer. SHEs have short lifetimes and the SHE production cross sections in various reactions are extremely low; therefore it is very difficult to study various properties of SHEs. Many experimental groups in various institutes—Grand Accélérateur National D'Ions Lourds, GSI Helmholtzzentrum für Schwerionenforschung GmbH, Institute of Modern Physics, Japan Atomic Energy Agency, Joint Institute for Nuclear Research, Lawrence Berkeley National Laboratory, RIKEN, and the Department of Physics of University of Jyväskylä—are studying various peculiarities of SHEs (see Refs. [1–16] and references cited therein).

To produce SHEs in experiments, there are two reaction types: a hot fusion, based on heavy actinide targets and light projectile nuclei, and a cold fusion, based on usage of lead or bismuth targets and light projectile nuclei. The heaviest nucleus that has been formed in a hot fusion reaction is ^{294}118 [10]. The heaviest nucleus produced in a cold fusion reaction is ^{278}113 [14]. The lifetimes and the production cross sections of these elements are close to 0.34 ms, 0.5 pb and 0.89 ms, 0.055 pb, respectively [10,14]. These experiments lasted several months.

Compound nuclei formed in fusion reactions leading to SHEs are in the highly exited states. The formed compound nucleus is unstable. The main decay channels of a compound nucleus are fission and neutron emission. An excited compound nucleus is cooling down during neutron emission. The excitation energy of compound nuclei formed by cold fusion reactions Ca, Ti, Cr, Fe, Ni, Ge + Pb, or Bi is a relatively low, approximately 10–20 MeV [1,7,11,17]. Therefore, one to two neutrons are emitted in this type of reactions. In case of the hot fusion processes induced by ^{48}Ca + U, Pu, Am, Cm, Bk, or Cf, the values of the excitation energy can reach 30–50 MeV and three to five emitted neutrons are observed [1,7,11,18].

When the excitation energy becomes smaller than the threshold of neutron emission, the γ quanta are emitted from the compound nucleus [16,17]. The SHE in the ground state is formed at the end of the cooling-down process of the compound nucleus. The α particles are mainly emitted from the ground state of a formed SHE, because, as a rule, the γ-decay half-lives of low-lying excitation states are shorter than the α-decay half-lives of corresponding levels. However, it is necessary to stress that α transitions can proceed between the ground state of a formed SHE and both the ground and the excited states of the daughter nucleus. A SHE can decay by fission, too. The main decay mode of a SHE is determined by the ratio between fission and α-decay half-lives. The chains of emitted α particles and/or fission fragments observed in experiment [1,3–14] are the evidence of a SHE formed during nucleus-nucleus fusion reaction. Therefore, it is very important to estimate the half-lives of such SHEs for designing experiments. There are many works devoted to the fission half-lives and fission barrier calculation (see Refs. [19–25] and references cited therein). The α-decay half-lives are extensively discussed also (see Refs. [26–36] and articles cited therein).

Recently, the α-decay half-lives between ground states for 344 α emitters and the α-capture cross sections of ^{40}Ca, ^{44}Ca, ^{59}Co, ^{208}Pb, and ^{209}Bi have been well described in the framework of the unified model for α decay and α capture (UMADAC) [37]. The experimental data for α-decay half-lives to ground and excited states of deformed nuclei with $222 \leqslant A \leqslant 252$ and $88 \leqslant Z \leqslant 102$ are also analyzed in the framework of the UMADAC [38]. Furthermore, the α-decay half-lives between ground states for 344 α emitters are considered with the help of sets of simple empirical equations [39]. The resulting sets of simple expressions well describe the whole data set, as well as the heavy and light subsets of nuclei separately. Because of this it is interesting to estimate the α-decay half-lives between the ground states of even-even SHEs within the range of proton number $104 \leqslant Z \leqslant 126$ in the framework of approaches proposed in Refs. [37–39].

The approaches proposed in Refs. [37–39] used the α-decay Q values from the table of evaluated atomic masses in Ref. [40]. However, the evaluated data for masses of nuclei with number of protons $Z > 118$ are not presented in Ref. [40] owing to the lack of any experimental information. Therefore, we extract the α-decay Q values between the ground states by using various approximations to atomic masses [41–46] if values of atomic masses are not given in Ref. [40].

Section II is devoted to a short description of our approaches [37–39]. The evaluation and discussion of the α-decay half-lives of SHEs with $104 \leqslant Z \leqslant 126$ are given in Sec. III.

II. THEORETICAL APPROACHES

To calculate corresponding α-decay half-lives we, use approaches proposed in Refs. [37–39].

The α-decay half-life $T_{1/2}$ evaluated in the framework of the UMADAC [37,38] is

$$T_{1/2} = \frac{\hbar \ln(2)}{\Gamma} = \frac{\hbar \ln(2)}{\frac{1}{4\pi}\int \gamma(\theta,\phi) d\Omega}. \quad (1)$$

Here Γ is the total α-decay width, which is expressed through the averaging of the partial widths $\gamma(\theta, \phi)$ of α emission in direction θ and ϕ, Ω is the space angle. Using this averaging on space angle, we can take into account the influence of nuclear shape deformation of a daughter nucleus on the α-transition.

The partial width of α emission is proportional to both the α-particle frequency assaults on the barrier ν (which takes into account the α-particle preformation too) and the transmission coefficient $t(Q_\alpha, \theta, \ell)$, which shows the probability of penetration through the barrier [37,38]; that is,

$$\gamma(\theta) = \hbar\ 10^{\nu}\ t(Q_\alpha, \theta, \ell). \quad (2)$$

The transmission coefficient is obtained in the semiclassical WKB approximation

$$t(Q_\alpha, \theta, \ell) = \left(1 + \exp\left\{\frac{2}{\hbar}\int_{a(\theta)}^{b(\theta)} dr \sqrt{2M\left[v(r,\theta,\ell,Q_\alpha) - Q_\alpha\right]}\right\}\right)^{-1}. \quad (3)$$

Here $a(\theta)$ and $b(\theta)$ are the inner and outer turning points, respectively, determined from the equations $v(r, \theta, \ell, Q_\alpha)|_{r=a(\theta),b(\theta)} = Q_\alpha$, M is the reduced mass, $v(r, \theta, \ell, Q_\alpha)$ is the total α-nucleus potential (see for details in Refs. [37,38]), ℓ is the orbital momentum of the α particle, and

$$Q_\alpha = M_{Z,N} - M_{Z-2,N-2} - M_{2,2} \quad (4)$$

is the released energy at the α decay of naked (without electron shells) nuclei [47], which is related to the masses of parent, daughter, and ^{4}He nuclei. The mass of the nucleus (in MeV) with Z protons and N neutrons can be found from the mass excess $\Delta\mathcal{M}_{Z,N}$ by use of the relationship [48]

$$M_{Z,N} = (Z+N)u + \Delta\mathcal{M}_{Z,N} - Zm_e + kZ^\epsilon. \quad (5)$$

Here the value $u = 931.5014$ MeV, $m_e = 0.510\,999\,06$ MeV is the mass of the electron [48], kZ^ϵ represents the energy of bound Z electrons in the atom, $k = 8.7$ eV and $\epsilon = 2.517$ for nuclei with $Z \geqslant 60$, and $k = 13.6$ eV and $\epsilon = 2.408$ for nuclei with $Z < 60$ [37,49].

Note that evaluated values of atomic mass excess $\Delta\mathcal{M}_{Z,N}$ are given in Ref. [40]. The released energy at the α decay of an atom [40], which can be evaluated in experiments, is

$$Q^0_\alpha = \Delta\mathcal{M}_{Z,N} - (\Delta\mathcal{M}_{Z-2,N-2} + \Delta\mathcal{M}_{2,2}), \quad (6)$$

where $\Delta\mathcal{M}_{Z,N}$, $\Delta\mathcal{M}_{Z-2,N-2}$, and $\Delta\mathcal{M}_{2,2}$ are, correspondingly, the mass excess of parent, daughter, and ^{4}He atoms.

The energy of bound electrons changes during α decay, too. The processes with participation of the electron shell occur after α-particle emission from nucleus. The recoiling nucleus is very quickly stripped of two electrons to neutralize the ionized helium cation (^{4}He nucleus). However, the α-nucleus interaction and Q_α determine the half-life of α decay in Eqs. (1)–(3) only (see also [47]). Therefore, the energy correction effect related to atomic bound electrons on Q_α should be taken into account [37,38,49]:

$$Q_\alpha = \Delta\mathcal{M}_{Z,N} - (\Delta\mathcal{M}_{Z-2,N-2} + \Delta\mathcal{M}_{2,2}) + k[Z^\epsilon - (Z-2)^\epsilon] = Q^0_\alpha + k[Z^\epsilon - (Z-2)^\epsilon]. \quad (7)$$

Here we neglect by the contribution of α-particle electrons because it is very small. In this case, Q_α in Eqs. (4) and (7) and all physical quantities in Eq. (3) are related to the α-nucleus system and the effect of electron shells is excluded. Note that the value of the second term in Eq. (7) is, as a rule, much smaller than the first one; however, it should be taken into account because of exponential dependence of transmission coefficient on Q_α in accurate approaches for α-decay.

The other approaches relate to the empirical relationships for α-decay half-lives [39]:

$$\log_{10}(T_{1/2}) = a_1 + a_2(A-4)^{1/6}Z^{1/2} + \frac{a_3 Z}{\sqrt{Q_\alpha}} + \frac{a_4\sqrt{\ell(\ell+1)}}{Q_\alpha A^{-1/6}} + a_5[(-1)^\ell - 1]. \quad (8)$$

Here A and Z are the mass number and charge of the parent nucleus, respectively, and ℓ is the orbital moment of emitted α particle. The value of $T_{1/2}$ is given in seconds and the reaction energy Q_α in MeV. The resulting sets of parameters a_i ($i = 1, 2, \ldots 5$) are obtained for the whole data set (344 α transitions between the ground states) for heavy (with $A - Z > 126$ and $Z > 82$) and light (rest part of nuclei from the full set) nuclei separately. Such empirical relations are very accurate in dedicated ranges of nuclei. The α-particle orbital moment and parity terms are introduced for transitions in even-odd, odd-even, and odd-odd nuclei. The electron screening effect is also taken into account.

We stress that both our approaches directly take into account the angular momentum of α-transition ℓ. So we can easily apply them for even-odd, odd-even, and odd-odd nuclei. However, systematic studies (even theoretical) of the ground-state spins for even-odd, odd-even, and odd-odd SHEs with $Z > 110$ have yet to be undertaken. Therefore, we limit our studies to α-decay half-lives between ground states in even-even SHEs only because the ground-state spins and parities of even-even nuclei are 0^+. As a result, the orbital moment of an emitted α particle at α transition between ground states of even-even parent and daughter nuclei is well-known: $\ell = 0$.

III. DESCRIPTION OF THE CALCULATION

The difference between the nucleus-nucleus fusion barrier and the ground-state energy of the compound nucleus formed in cold and hot fusion reactions reduces with increasing mass of projectiles [18]; therefore, the reasonable number of evaporated neutrons is 0-1-2 for cold fusion reactions and 0-1-2-3-4 for hot fusion reactions. So we consider α-decay in

TABLE I. The comparison of the experimental α-decay half-lives with different forms of the empirical relations (ERTR, empirical relations for total range of nuclei; ERHR, empirical relations for heavy range of nuclei).

A	Z	$Q_\alpha^{\rm exp}$ (MeV)	Ref.	$T_{1/2}^{\rm exp}$	$T_{1/2}$ [37]	$T_{1/2}^{\rm ERTR}$ [39]	$T_{1/2}^{\rm ERHR}$ [39]	$T_{1/2}$ [30]	$T_{1/2}$ [34]
256	104	8.996	[36]	0.304 s	1.538 s	1.022 s	1.150 s	1.040 s	0.653 s
258	104	9.296	[34]	$92^{+15.3}_{-15.3}$ ms	184 ms	116 ms	135 ms	141 ms	76 ms
260	104	8.947	[34]	$1^{+0.035}_{-0.035}$ s	2.340 s	1.214 s	1.381 s	1.455 s	0.773 s
264	108	10.848	[36]	0.081 ms	0.439 ms	0.182 ms	0.261 ms	0.300 ms	0.126 ms
266	108	10.388	[34]	2.3 ms	6.219 ms	2.377 ms	3.304 ms	3.805 ms	1.584 ms
270	108	9.068	[34]	22 s	33.778 s	12.161 s	15.228 s	15.919 s	7.257 s
270	110	11.284	[3]	$0.100^{+0.14}_{-0.04}$ ms	0.175 ms	0.063 ms	0.097 ms	0.123 ms	0.043 ms
284	112	9.286	[12]	9.8 s	303.62 s	49.177 s	69.374 s	84.462 s	27.769 s
286	114	10.382	[10]	$0.26^{+0.04}_{-0.02}$ s	0.956 s	0.148 s	0.238 s	0.311 s	0.088 s
288	114	10.132	[11]	$0.80^{+0.27}_{-0.16}$ s	4.276 s	0.675 s	1.072 s	1.445 s	0.396 s
290	116	11.054	[10]	$7.1^{+3.2}_{-1.7}$ ms	38.092 ms	10.782 ms	19.093 ms	26.228 ms	6.549 ms
292	116	10.854	[11]	$0.018^{+0.016}_{-0.006}$ s	0.221 s	0.032 s	0.057 s	0.814 s	0.019 s
294	118	11.865	[10]	$0.89^{+1.07}_{-0.31}$ ms	3.163 ms	0.464 ms	0.911 ms	1.3290 ms	0.289 ms

even-even SHEs formed in cold and hot fusion reactions after possible emissions of 0-1-2-3-4 neutrons.

First, we compare the α-decay half-lives between ground states in even-even SHEs evaluated in the framework of three of our approaches (UMADAC [37], empirical relations for total range of nuclei (ERTR) [39], and empirical relations for heavy range of nuclei (ERHR) [39]), with available experimental data in Table I. The α-decay half-lives obtained in the framework of other approaches [30,34] are also presented in Table I. Note that various α-decay data presented in Table I have been analyzed by other authors, too [26–36]. The theoretical values of α-decay half-lives presented in Table I agree with the experimental ones.

Comparing results obtained in the framework of our approaches, we can conclude that the values of half-lives evaluated in the UMADAC are the longest ones, while the values of half-lives obtained by using the ERTR are the shortest ones.

However, the shortest half-life values for each SHE presented in Table I are evaluated using empirical relations from Ref. [34]. The values of half-lives obtained by applying the empirical relations from Ref. [30] are close to the ones calculated by using ERHR [39]. It is no wonder, because the empirical relations in Ref. [30] are also obtained by fitting data for the heavy range of nuclei.

Further, we considered the fusion reactions between natural isotopes,

^{62}Ni, ^{64}Ni, ^{68}Zn, ^{70}Zn, ^{74}Ge, ^{76}Ge, ^{80}Se, ^{82}Se + ^{238}U;
^{56}Fe, ^{57}Fe, ^{58}Fe, ^{60}Ni, ^{62}Ni, ^{64}Ni, ^{68}Zn, ^{70}Zn, ^{74}Ge, ^{76}Ge + ^{244}Pu;
^{52}Cr, ^{53}Cr, ^{54}Cr, ^{56}Fe, ^{57}Fe, ^{58}Fe, ^{60}Ni, ^{62}Ni, ^{64}Ni, ^{68}Zn, ^{70}Zn + ^{248}Cm;
^{88}Sr, ^{86}Sr, ^{92}Zn, ^{90}Zn, ^{98}Mo, ^{96}Mo, ^{94}Mo, ^{104}Ru, ^{102}Ru, ^{100}Ru, ^{98}Ru + ^{208}Pb;
^{85}Rb, ^{89}Y, ^{93}Nb + ^{209}Bi,

and calculated the corresponding α-decay half-life values of the produced nuclei, as well as the nuclei of their α-decay chains. The nuclei obtained after possible emission of zero, one, two, three, and four neutrons from produced compound nuclei and also nuclei of their α-decay chains are considered, too. The ranges of the mass numbers and charges for the new SHEs formed in these reactions are, correspondingly, $292 \leqslant A \leqslant 318$ and $120 \leqslant Z \leqslant 126$. We stress that reactions ^{48}Ca + ^{238}U, ^{48}Ca + ^{244}Pu, ^{48}Ca + ^{248}Cm, ^{70}Ca + ^{208}Pb, and ^{70}Zn + ^{209}Bi have been successfully used for synthesis of corresponding SHEs [1,3–7,10–14]. The heaviest SHEs are synthesized in these reactions for corresponding target nuclei. The listed isotopes can be easy used in experiments because they are available in nature. Of greatest natural abundance (100%) from the listed isotopes are ^{89}Y and ^{93}Nb, and the least-abundant one (0.282%) is ^{58}Fe. However, more heavy even-even target nuclei are practically unavailable for experiments in the case of hot fusion reactions owing to very high radioactivity and/or lack in nature. Note that nuclei considered by proposed reactions can be also obtained by other combinations of projectile-target nuclei; therefore, these SHEs cover a wide range of nuclei, which may be related to future experiments.

We present only α transitions between the ground states of even-even nuclei, produced in all fusion reactions listed in Table II.

Because there are no experimental data of the masses of SHEs within the ranges $292 \leqslant A \leqslant 318$ and $120 \leqslant Z \leqslant 126$, it is necessary to evaluate the α-decay Q values to calculate the corresponding values of the α-decay half-lives. We consider different mass formulas [41–45] and results presented in Ref. [46] for determination of Q values. The corresponding Q values and relating half-lives evaluated in the framework of the UMADAC, ERTR, and ERHR are presented in Table II. There are no data of the α-decay half-lives for considered SHEs; therefore, it is useful to compare our results (UMADAC, ERTR, and ERHR) with the ones obtained in the framework of other approaches [30,34].

Visualization of results for the α-decay half-lives evaluated by using the ERHR and Q values obtained from different approaches is given in Fig. 1. Detailed numerical comparison can be found in Table II; however, results presented in Fig. 1

TABLE II. The comparison of the α-decay half-lives in different empirical approaches for Q values calculated in the framework of the different mass formulas.

Nucleus	Q_α (MeV)		$T_{1/2}$ [37]	$T_{1/2}^{\mathrm{ERTR}}$ [39]	$T_{1/2}^{\mathrm{ERHR}}$ [39]	$T_{1/2}$ [30]	$T_{1/2}$ [34]
^{264}106	8.465	[41]	6.66×10^{2} s	2.48×10^{2} s	2.79×10^{2} s	2.50×10^{2} s	1.45×10^{2} s
	8.756	[42]	67.25 s	25.95 s	30.08 s	28.76 s	15.62 s
	8.936	[43]	17.29 s	6.78 s	8.01 s	7.97 s	4.15 s
	9.536	[44]	0.25 s	0.10 s	0.13 s	0.14 s	0.07 s
	8.996	[45]	11.10 s	6.35 s	7.51 s	5.24 s	2.70 s
^{266}106	7.725	[41]	3.94×10^{5} s	1.25×10^{5} s	1.30×10^{5} s	1.04×10^{5} s	0.68×10^{5} s
	8.076	[42]	16.52×10^{3} s	5.62×10^{3} s	6.09×10^{3} s	5.37×10^{3} s	3.16×10^{3} s
	8.256	[43]	3.53×10^{3} s	1.24×10^{3} s	1.37×10^{3} s	1.26×10^{3} s	0.71×10^{3} s
	9.327	[44]	0.98 s	0.39 s	0.48 s	0.56 s	0.24 s
	8.476	[45]	5.74×10^{2} s	3.13×10^{2} s	3.53×10^{2} s	2.30×10^{2} s	1.22×10^{2} s
^{268}106	7.545	[41]	21.73×10^{5} s	6.10×10^{5} s	6.23×10^{5} s	5.17×10^{5} s	3.23×10^{5} s
	7.646	[42]	8.22×10^{5} s	2.37×10^{5} s	2.45×10^{5} s	2.09×10^{5} s	1.27×10^{5} s
	7.816	[43]	16.76×10^{4} s	5.02×10^{4} s	5.31×10^{4} s	4.74×10^{4} s	2.74×10^{4} s
	9.107	[44]	4.56 s	1.65 s	2.01 s	2.44 s	1.03 s
	7.946	[45]	5.15×10^{4} s	2.48×10^{4} s	2.65×10^{4} s	1.58×10^{4} s	0.88×10^{4} s
^{270}106	7.385	[41]	8.90×10^{6} s	2.60×10^{6} s	2.63×10^{6} s	2.25×10^{6} s	1.35×10^{6} s
	8.206	[42]	4.47×10^{3} s	1.58×10^{3} s	1.76×10^{3} s	1.88×10^{3} s	0.90×10^{3} s
	8.396	[43]	9.14×10^{2} s	3.32×10^{2} s	3.79×10^{2} s	4.24×10^{2} s	1.93×10^{2} s
	8.877	[44]	20.90 s	8.05 s	9.67 s	12.08 s	4.91 s
	8.786	[45]	41.67 s	23.39 s	27.68 s	23.16 s	9.61 s
^{272}106	7.245	[41]	35.60×10^{6} s	9.56×10^{6} s	9.53×10^{6} s	8.50×10^{6} s	4.88×10^{6} s
	8.436	[42]	6.30×10^{2} s	2.21×10^{2} s	2.55×10^{2} s	3.12×10^{2} s	1.29×10^{2} s
	8.616	[43]	148.78 s	53.5 s	62.96 s	80.23 s	31.80 s
	8.631	[44]	132.12 s	47.57 s	56.11 s	71.75 s	28.33 s
	8.546	[45]	2.59×10^{2} s	1.38×10^{2} s	1.60×10^{2} s	1.35×10^{2} s	0.55×10^{2} s
^{274}106	7.155	[41]	9.50×10^{7} s	2.19×10^{7} s	2.17×10^{7} s	2.04×10^{7} s	1.10×10^{7} s
	8.366	[42]	11.53×10^{2} s	3.56×10^{2} s	4.11×10^{2} s	5.34×10^{2} s	2.06×10^{2} s
	8.546	[43]	2.67×10^{2} s	0.85×10^{2} s	1.00×10^{2} s	1.35×10^{2} s	0.5×10^{2} s
	8.367	[44]	11.43×10^{2} s	3.53×10^{2} s	4.07×10^{2} s	5.30×10^{2} s	2.05×10^{2} s
	8.176	[45]	5.71×10^{3} s	2.62×10^{3} s	2.94×10^{3} s	2.39×10^{3} s	0.97×10^{3} s
^{268}108	8.645	[41]	9.70×10^{2} s	3.29×10^{2} s	3.91×10^{2} s	3.43×10^{2} s	1.88×10^{2} s
	9.047	[42]	43.60 s	15.52 s	19.24 s	18.48 s	9.24 s
	9.248	[43]	10.03 s	3.63 s	4.60 s	4.61 s	2.20 s
	10.208	[44]	17.27 ms	6.49 ms	8.95 ms	10.82 ms	4.26 ms
	9.548	[45]	1.23 s	0.65 s	0.84 s	0.63 s	0.28 s
^{272}108	8.305	[41]	12.75×10^{3} s	4.33×10^{3} s	5.04×10^{3} s	4.78×10^{3} s	2.40×10^{3} s
	9.258	[42]	7.38 s	2.84 s	3.65 s	4.31 s	1.73 s
	9.438	[43]	2.07 s	0.81 s	1.06 s	1.29 s	0.50 s
	9.768	[44]	22.25×10^{-2} s	8.83×10^{-2} s	11.90×10^{-2} s	15.55×10^{-2} s	56.03×10^{-2} s
	9.848	[45]	13.20×10^{-2} s	7.38×10^{-2} s	9.98×10^{-2} s	9.46×10^{-2} s	3.35×10^{-2} s
^{274}108	8.175	[41]	3.76×10^{4} s	1.19×10^{4} s	1.37×10^{4} s	1.37×10^{4} s	0.65×10^{4} s
	9.518	[42]	1.14 s	0.43 s	0.57 s	0.77 s	0.27 s
	9.698	[43]	0.34 s	0.13 s	0.17 s	0.24 s	0.08 s
	9.524	[44]	1.10 s	0.41 s	0.55 s	0.74 s	0.26 s
	9.608	[45]	0.62 s	0.33 s	0.44 s	0.43 s	0.15 s
^{276}108	8.085	[41]	8.65×10^{4} s	2.37×10^{4} s	2.73×10^{4} s	2.87×10^{4} s	1.28×10^{4} s
	9.378	[42]	3.10 s	1.03 s	1.36 s	1.92 s	0.63 s
	9.568	[43]	0.83 s	0.28 s	0.38 s	0.55 s	0.17 s
	9.259	[44]	7.26 s	2.38 s	3.11 s	4.29 s	1.45 s
	9.248	[45]	7.86 s	3.74 s	4.86 s	4.62 s	1.56 s
^{278}108	8.115	[41]	7.83×10^{4} s	1.68×10^{4} s	1.95×10^{4} s	2.24×10^{4} s	0.91×10^{4} s
	8.578	[42]	15.37×10^{2} s	3.62×10^{2} s	4.44×10^{2} s	5.69×10^{2} s	2.06×10^{2} s
	8.778	[43]	31.16×10^{1} s	7.58×10^{1} s	9.49×10^{1} s	12.77×10^{1} s	4.40×10^{1} s
	8.964	[44]	74.58 s	18.63 s	23.79 s	33.34 s	11.02 s
	8.818	[45]	22.89×10^{1} s	8.38×10^{1} s	10.48×10^{1} s	9.56×10^{1} s	3.27×10^{1} s

TABLE II. (*Continued.*)

Nucleus	Q_α (MeV)		$T_{1/2}$ [37]	$T_{1/2}^{\mathrm{ERTR}}$ [39]	$T_{1/2}^{\mathrm{ERHR}}$ [39]	$T_{1/2}$ [30]	$T_{1/2}$ [34]
^{280}108	8.035	[41]	17.90×10^4 s	3.10×10^4 s	3.59×10^4 s	4.36×10^4 s	1.67×10^4 s
	7.617	[42]	9.14×10^6 s	1.41×10^6 s	1.55×10^6 s	1.68×10^6 s	0.72×10^6 s
	7.808	[43]	14.54×10^5 s	2.37×10^5 s	2.67×10^5 s	3.05×10^5 s	1.24×10^5 s
	8.632	[44]	11.08×10^2 s	2.17×10^2 s	2.70×10^2 s	3.80×10^2 s	1.25×10^2 s
	8.058	[45]	14.62×10^4 s	4.03×10^4 s	4.66×10^4 s	3.61×10^4 s	1.37×10^4 s
^{272}110	9.415	[41]	15.69 s	5.53 s	7.39 s	7.21 s	3.28 s
	10.089	[42]	16.64×10^{-2} s	6.11×10^{-2} s	8.67×10^{-2} s	9.67×10^{-2} s	3.83×10^{-2} s
	10.279	[43]	50.42 ms	18.58 ms	26.83 ms	30.97 ms	11.84 ms
	10.874	[44]	14.95×10^{-4} s	5.49×10^{-4} s	8.32×10^{-4} s	10.65×10^{-4} s	3.66×10^{-4} s
	10.789	[45]	2.43 ms	1.22 ms	1.83 ms	1.70 ms	0.59 ms
^{274}110	9.265	[41]	39.70 s	14.77 s	19.59 s	20.05 s	8.64 s
	10.559	[42]	7.93 ms	3.13 ms	4.66 ms	6.12 ms	2.04 ms
	10.769	[43]	2.33 ms	0.92 ms	1.39 ms	1.89 ms	0.61 ms
	10.651	[44]	4.61 ms	1.82 ms	2.73 ms	3.64 ms	1.19 ms
	11.629	[45]	22.77 μs	11.31 μs	18.19 μs	24.64 μs	6.01 μs
^{276}110	9.135	[41]	98.07 s	34.94 s	46.08 s	49.66 s	20.20 s
	10.779	[42]	2.07 ms	0.79 ms	1.21 ms	1.79 ms	0.51 ms
	10.979	[43]	6.71×10^{-4} s	2.55×10^{-4} s	3.96×10^{-4} s	6.05×10^{-4} s	1.71×10^{-4} s
	10.408	[44]	18.45 ms	7.08 ms	10.50 ms	14.55 ms	4.56 ms
	11.139	[45]	2.79×10^{-4} s	1.42×10^{-4} s	2.22×10^{-4} s	2.59×10^{-4} s	0.72×10^{-4} s
^{278}110	9.035	[41]	198.05 s	67.37 s	88.61 s	101.09 s	38.59 s
	10.459	[42]	12.84 ms	4.78 ms	7.16 ms	10.84 ms	3.09 ms
	10.659	[43]	3.93 ms	1.46 ms	2.22 ms	3.49 ms	0.96 ms
	10.139	[44]	92.54 ms	34.25 ms	49.99 ms	71.37 ms	21.60 ms
	10.599	[45]	5.58 ms	2.86 ms	4.31 ms	4.88 ms	1.36 ms
^{280}110	9.205	[41]	71.40 s	17.61 s	23.73 s	30.40 s	10.25 s
	9.099	[42]	157.85 s	38.37 s	51.17 s	64.05 s	22.12 s
	9.299	[43]	35.76 s	8.92 s	12.14 s	15.87 s	5.24 s
	9.839	[44]	0.83 s	0.22 s	0.31 s	0.45 s	0.13 s
	9.969	[45]	0.35 s	0.13 s	0.19 s	0.20 s	0.06 s
^{282}110	9.125	[41]	170.42 s	29.06 s	39.15 s	52.29 s	16.80 s
	7.809	[42]	12.66×10^6 s	1.59×10^6 s	1.84×10^6 s	1.82×10^6 s	0.80×10^6 s
	7.999	[43]	20.98×10^5 s	2.79×10^5 s	3.32×10^5 s	3.44×10^5 s	1.44×10^5 s
	9.500	[44]	11.02 s	1.98 s	2.77 s	4.08 s	1.18 s
	8.939	[45]	7.09×10^2 s	1.77×10^2 s	2.33×10^2 s	2.02×10^2 s	0.67×10^2 s
^{284}110	9.165	[41]	110.75 s	19.89 s	27.10 s	40.21 s	11.54 s
	7.619	[42]	71.81×10^6 s	8.88×10^6 s	10.12×10^6 s	10.22×10^6 s	4.37×10^6 s
	7.819	[43]	10.08×10^6 s	1.33×10^6 s	1.56×10^6 s	1.66×10^6 s	0.67×10^6 s
	9.110	[44]	167.41 s	29.81 s	40.40 s	59.22 s	17.21 s
	8.389	[45]	5.63×10^4 s	1.37×10^4 s	1.71×10^4 s	1.35×10^4 s	0.47×10^4 s
^{286}110	9.225	[41]	62.82 s	11.80 s	16.29 s	26.45 s	6.88 s
	7.659	[42]	42.57×10^6 s	5.55×10^6 s	6.41×10^6 s	7.07×10^6 s	2.75×10^6 s
	7.859	[43]	60.73×10^5 s	8.44×10^5 s	1.00×10^6 s	11.67×10^5 s	4.28×10^5 s
	8.656	[44]	52.83×10^2 s	8.99×10^2 s	11.69×10^2 s	16.71×10^2 s	4.97×10^2 s
	8.039	[45]	11.24×10^5 s	2.67×10^5 s	3.22×10^5 s	2.44×10^5 s	0.85×10^5 s
^{276}112	10.225	[41]	0.32 s	0.12 s	0.17 s	0.19 s	0.07 s
	11.901	[42]	25.54 μs	8.96 μs	15.25 μs	21.63 μs	6.18 μs
	12.101	[43]	9.58 μs	3.31 μs	5.70 μs	8.34 μs	2.31 μs
	11.527	[44]	17.27×10^{-5} s	6.20×10^{-5} s	10.28×10^{-5} s	13.78×10^{-5} s	4.18×10^{-5} s
	12.281	[45]	4.07 μs	1.80 μs	3.14 μs	3.61 μs	0.98 μs
^{278}112	10.095	[41]	0.65 s	0.24 s	0.36 s	0.41 s	0.15 s
	12.351	[42]	2.57 μs	0.9 μs	1.59 μs	2.61 μs	0.64 μs
	12.541	[43]	10.70×10^{-7} s	3.68×10^{-7} s	6.58×10^{-7} s	11.09×10^{-7} s	2.64×10^{-7} s
	11.283	[44]	5.57×10^{-4} s	2.11×10^{-4} s	3.46×10^{-4} s	4.84×10^{-4} s	1.40×10^{-4} s
	11.911	[45]	2.14×10^{-5} s	1.04×10^{-5} s	1.77×10^{-5} s	2.07×10^{-5} s	0.54×10^{-5} s
^{280}112	9.985	[41]	1.33 s	0.46 s	0.68 s	0.82 s	0.28 s
	11.181	[42]	9.68×10^{-4} s	3.39×10^{-4} s	5.56×10^{-4} s	8.26×10^{-4} s	2.23×10^{-4} s

TABLE II. (*Continued.*)

Nucleus	Q_α (MeV)		$T_{1/2}$ [37]	$T_{1/2}^{\mathrm{ERTR}}$ [39]	$T_{1/2}^{\mathrm{ERHR}}$ [39]	$T_{1/2}$ [30]	$T_{1/2}$ [34]
	11.391	[43]	3.10×10^{-4} s	1.08×10^{-4} s	1.79×10^{-4} s	2.75×10^{-4} s	0.72×10^{-4} s
	11.009	[44]	2.54 ms	0.89 ms	1.44 ms	2.08 ms	0.58 ms
	11.461	[45]	2.14×10^{-4} s	1.00×10^{-4} s	1.66×10^{-4} s	1.93×10^{-4} s	0.50×10^{-4} s
$^{282}112$	10.305	[41]	23.14×10^{-2} s	5.41×10^{-2} s	8.33×10^{-2} s	11.50×10^{-2} s	3.33×10^{-2} s
	9.470	[42]	65.56 s	14.21 s	20.26 s	23.72 s	8.16 s
	9.671	[43]	15.68 s	3.48 s	5.06 s	6.18 s	2.03 s
	10.700	[44]	20.61 ms	4.90 ms	7.79 ms	1.15 ms	3.11 ms
	10.741	[45]	16.17 ms	5.34 ms	8.48 ms	9.16 ms	2.45 ms
$^{284}112$	10.235	[41]	42.56×10^{-2} s	7.72×10^{-2} s	11.90×10^{-2} s	17.53×10^{-2} s	4.73×10^{-2} s
	8.751	[42]	20.19×10^{3} s	2.95×10^{3} s	3.94×10^{3} s	4.25×10^{3} s	1.58×10^{3} s
	8.941	[43]	43.46×10^{2} s	6.61×10^{2} s	9.00×10^{2} s	10.15×10^{2} s	3.61×10^{2} s
	10.347	[44]	20.95×10^{-2} s	3.83×10^{-2} s	5.96×10^{-2} s	8.97×10^{-2} s	2.37×10^{-2} s
	9.811	[45]	7.09 s	1.80 s	2.65 s	2.49 s	0.73 s
$^{286}112$	10.265	[41]	31.58×10^{-2} s	5.86×10^{-2} s	9.13×10^{-2} s	14.62×10^{-2} s	3.60×10^{-2} s
	8.541	[42]	10.52×10^{4} s	1.50×10^{4} s	1.97×10^{4} s	2.18×10^{4} s	0.79×10^{4} s
	8.731	[43]	21.34×10^{3} s	3.18×10^{3} s	4.27×10^{3} s	4.95×10^{3} s	1.70×10^{3} s
	9.943	[44]	2.60 s	0.47 s	0.71 s	1.07 s	0.28 s
	9.401	[45]	116.64 s	29.38 s	42.01 s	38.16 s	11.24 s
$^{288}112$	10.315	[41]	20.59×10^{-2} s	3.94×10^{-2} s	6.20×10^{-2} s	10.83×10^{-2} s	2.43×10^{-2} s
	8.401	[42]	31.68×10^{4} s	4.47×10^{4} s	5.82×10^{4} s	6.73×10^{4} s	2.31×10^{4} s
	8.601	[43]	56.64×10^{3} s	8.41×10^{3} s	11.19×10^{3} s	13.60×10^{3} s	4.44×10^{3} s
	9.475	[44]	60.88 s	10.65 s	15.54 s	23.00 s	6.12 s
	9.101	[45]	10.01×10^{2} s	2.51×10^{2} s	3.51×10^{2} s	3.16×10^{2} s	0.92×10^{2} s
$^{290}112$	10.405	[41]	9.75×10^{-2} s	2.07×10^{-2} s	3.31×10^{-2} s	6.34×10^{-2} s	1.29×10^{-2} s
	7.701	[42]	18.63×10^{7} s	2.37×10^{7} s	2.84×10^{7} s	2.94×10^{7} s	1.13×10^{7} s
	7.901	[43]	25.99×10^{6} s	3.54×10^{6} s	4.36×10^{6} s	4.77×10^{6} s	1.73×10^{6} s
	8.931	[44]	31.40×10^{2} s	5.56×10^{2} s	7.73×10^{2} s	10.97×10^{2} s	3.04×10^{2} s
	9.041	[45]	13.21×10^{2} s	3.65×10^{2} s	5.11×10^{2} s	4.88×10^{2} s	1.32×10^{2} s
$^{280}114$	12.025	[41]	5.26×10^{-5} s	1.81×10^{-5} s	3.23×10^{-5} s	4.39×10^{-5} s	1.21×10^{-5} s
	11.662	[42]	3.37×10^{-4} s	1.18×10^{-4} s	2.06×10^{-4} s	2.65×10^{-4} s	0.78×10^{-4} s
	11.882	[43]	10.82×10^{-5} s	3.75×10^{-5} s	6.64×10^{-5} s	8.82×10^{-5} s	2.50×10^{-5} s
	12.141	[44]	2.96×10^{-5} s	1.01×10^{-5} s	1.82×10^{-5} s	2.51×10^{-5} s	0.68×10^{-5} s
	12.592	[45]	3.45 μs	1.48 μs	2.75 μs	3.10 μs	0.79 μs
$^{282}114$	11.995	[41]	8.05×10^{-5} s	1.93×10^{-5} s	3.47×10^{-5} s	5.07×10^{-5} s	1.29×10^{-5} s
	10.062	[42]	6.02 s	1.39 s	2.14 s	2.25 s	0.81 s
	10.272	[43]	1.51 s	0.35 s	0.56 s	0.61 s	0.21 s
	11.857	[44]	16.22×10^{-5} s	3.91×10^{-5} s	6.96×10^{-5} s	9.97×10^{-5} s	2.60×10^{-5} s
	12.142	[45]	3.87×10^{-5} s	1.22×10^{-5} s	2.22×10^{-5} s	2.50×10^{-5} s	0.62×10^{-5} s
$^{284}114$	12.095	[41]	6.62×10^{-5} s	1.07×10^{-5} s	1.95×10^{-5} s	3.13×10^{-5} s	0.72×10^{-5} s
	9.492	[42]	481.25 s	65.06 s	95.80 s	97.00 s	36.04 s
	9.692	[43]	112.57 s	15.73 s	23.61 s	24.94 s	8.87 s
	11.533	[44]	12.23×10^{-4} s	1.98×10^{-4} s	3.47×10^{-4} s	5.11×10^{-4} s	1.29×10^{-4} s
	11.582	[45]	9.40×10^{-4} s	2.07×10^{-4} s	3.62×10^{-4} s	3.98×10^{-4} s	0.99×10^{-4} s
$^{286}114$	11.655	[41]	57.97×10^{-5} s	9.47×10^{-5} s	16.87×10^{-5} s	27.42×10^{-5} s	6.21×10^{-5} s
	9.452	[42]	5.83×10^{2} s	0.80×10^{2} s	1.18×10^{2} s	1.28×10^{2} s	0.44×10^{2} s
	9.662	[43]	125.86 s	17.81 s	26.86 s	30.49 s	10.02 s
	11.163	[44]	8.63 ms	1.40 ms	2.40 ms	3.60 ms	0.89 ms
	10.912	[45]	36.96 ms	8.28 ms	13.88 ms	14.35 ms	3.69 ms
$^{288}114$	11.305	[41]	3.41 ms	0.58 ms	1.01 ms	1.69 ms	0.37 ms
	9.222	[42]	29.15×10^{2} s	4.01×10^{2} s	5.83×10^{2} s	6.51×10^{2} s	2.17×10^{2} s
	9.442	[43]	5.50×10^{2} s	0.79×10^{2} s	1.17×10^{2} s	1.37×10^{2} s	0.43×10^{2} s
	10.739	[44]	9.11×10^{-2} s	1.51×10^{-2} s	2.53×10^{-2} s	3.82×10^{-2} s	0.93×10^{-2} s
	10.382	[45]	0.84 s	0.20 s	0.31 s	0.31 s	0.08 s
$^{290}114$	10.985	[41]	17.90 ms	3.27 ms	5.62 ms	9.56 ms	2.05 ms
	8.552	[42]	5.99×10^{5} s	0.77×10^{5} s	1.04×10^{5} s	1.07×10^{5} s	0.39×10^{5} s
	8.782	[43]	8.43×10^{4} s	1.14×10^{4} s	1.60×10^{4} s	1.74×10^{4} s	0.59×10^{4} s

TABLE II. (*Continued.*)

Nucleus	Q_α (MeV)		$T_{1/2}$ [37]	$T_{1/2}^{\mathrm{ERTR}}$ [39]	$T_{1/2}^{\mathrm{ERHR}}$ [39]	$T_{1/2}$ [30]	$T_{1/2}$ [34]
	10.251	[44]	1.66 s	0.29 s	0.46 s	0.69 s	0.17 s
	10.122	[45]	3.88 s	0.97 s	1.53 s	1.54 s	0.39 s
^{292}114	10.705	[41]	6.99×10^{-2} s	1.57×10^{-2} s	2.66×10^{-2} s	4.65×10^{-2} s	0.96×10^{-2} s
	8.312	[42]	38.10×10^{5} s	5.56×10^{5} s	7.42×10^{5} s	7.77×10^{5} s	2.74×10^{5} s
	8.522	[43]	58.38×10^{4} s	9.07×10^{4} s	12.40×10^{4} s	13.70×10^{4} s	4.57×10^{4} s
	9.689	[44]	57.03 s	11.41 s	17.65 s	25.43 s	6.44 s
	9.652	[45]	74.40 s	22.15 s	33.93 s	32.61 s	8.33 s
^{294}114	10.455	[41]	60.93×10^{-2} s	6.68×10^{-2} s	11.15×10^{-2} s	20.14×10^{-2} s	4.02×10^{-2} s
	8.672	[42]	30.70×10^{4} s	2.38×10^{4} s	3.33×10^{4} s	4.12×10^{4} s	1.22×10^{4} s
	8.892	[43]	48.60×10^{3} s	4.00×10^{3} s	5.74×10^{3} s	7.49×10^{3} s	2.09×10^{3} s
	9.039	[44]	14.74×10^{3} s	1.26×10^{3} s	1.84×10^{3} s	2.48×10^{3} s	067×10^{3} s
	9.162	[45]	55.68×10^{2} s	7.57×10^{2} s	11.12×10^{2} s	10.05×10^{2} s	2.63×10^{2} s
^{284}116	12.905	[41]	6.38 μs	0.93 μs	1.84 μs	2.65 μs	0.64 μs
	11.664	[42]	30.92×10^{-4} s	4.56×10^{-4} s	8.28×10^{-4} s	9.93×10^{-4} s	2.89×10^{-4} s
	11.884	[43]	9.57×10^{-4} s	1.42×10^{-4} s	2.61×10^{-4} s	3.25×10^{-4} s	0.91×10^{-4} s
	12.675	[44]	18.64 μs	2.74 μs	5.34 μs	7.45 μs	1.86 μs
	12.834	[45]	8.87 μs	1.71 μs	3.34 μs	3.64 μs	0.89 μs
^{286}116	12.685	[41]	16.55 μs	2.39 μs	4.70 μs	7.11 μs	1.62 μs
	11.474	[42]	8.16 ms	1.18 ms	2.12 ms	2.68 ms	0.74 ms
	11.704	[43]	23.18×10^{-4} s	3.37×10^{-4} s	6.19×10^{-4} s	8.09×10^{-4} s	2.14×10^{-4} s
	12.329	[44]	9.24×10^{-5} s	1.35×10^{-5} s	2.59×10^{-5} s	3.72×10^{-5} s	0.89×10^{-5} s
	12.454	[45]	50.10 μs	9.72 μs	18.72 μs	20.65 μs	4.87 μs
^{288}116	12.235	[41]	13.69×10^{-5} s	1.97×10^{-5} s	3.79×10^{-5} s	5.81×10^{-5} s	1.30×10^{-5} s
	11.374	[42]	13.24 ms	1.88 ms	3.40 ms	4.56 ms	1.17 ms
	11.604	[43]	36.98×10^{-4} s	5.31×10^{-4} s	9.73×10^{-4} s	13.54×10^{-4} s	3.35×10^{-4} s
	11.934	[44]	63.78×10^{-5} s	9.20×10^{-5} s	17.29×10^{-5} s	25.35×10^{-5} s	5.94×10^{-5} s
	11.604	[45]	3.71 ms	0.73 ms	1.34 ms	1.36 ms	0.34 ms
^{290}116	11.875	[41]	3.97×10^{-4} s	1.15×10^{-4} s	2.16×10^{-4} s	3.40×10^{-4} s	0.74×10^{-4} s
	11.174	[42]	18.88 ms	5.38 ms	9.61 ms	13.48 ms	3.29 ms
	11.394	[43]	5.39 ms	1.55 ms	2.81 ms	4.09 ms	0.96 ms
	11.482	[44]	3.31 ms	0.95 ms	1.74 ms	2.57 ms	0.60 ms
	11.144	[45]	22.53 ms	8.99 ms	15.96 ms	15.94 ms	3.92 ms
^{292}116	11.545	[41]	4.05 ms	0.62 ms	1.14 ms	1.84 ms	0.39 ms
	10.884	[42]	18.36×10^{-2} s	2.70×10^{-2} s	4.75×10^{-2} s	6.85×10^{-2} s	1.62×10^{-2} s
	11.083	[43]	56.02 ms	8.35 ms	14.94 ms	22.29 ms	5.09 ms
	10.969	[44]	11.04×10^{-2} s	1.63×10^{-2} s	2.89×10^{-2} s	4.23×10^{-2} s	0.99×10^{-2} s
	11.114	[45]	46.83 ms	9.83 ms	17.55 ms	18.82 ms	4.27 ms
^{294}116	11.245	[41]	27.99 ms	3.02 ms	5.51 ms	9.14 ms	1.86 ms
	11.034	[42]	9.63×10^{-2} s	1.02×10^{-2} s	1.83×10^{-2} s	2.93×10^{-2} s	0.62×10^{-2} s
	11.244	[43]	28.16 ms	3.04 ms	5.55 ms	9.19 ms	1.87 ms
	10.384	[44]	5.58 s	0.55 s	0.93 s	1.33 s	0.32 s
	10.804	[45]	0.39 s	0.06 s	0.10 s	0.11 s	0.02 s
^{296}116	10.965	[41]	12.14×10^{-2} s	1.41×10^{-2} s	2.53×10^{-2} s	4.32×10^{-2} s	0.85×10^{-2} s
	11.164	[42]	37.45 ms	4.42 ms	8.06 ms	14.24 ms	2.71 ms
	11.384	[43]	10.61 ms	1.27 ms	2.36 ms	4.32 ms	0.79 ms
	9.719	[44]	45.61×10^{1} s	4.46×10^{1} s	7.18×10^{1} s	9.65×10^{1} s	2.43×10^{1} s
	10.774	[45]	0.39 s	0.06 s	0.11 s	0.13 s	0.03 s
^{298}116	10.725	[41]	0.38 s	0.05 s	0.10 s	0.17 s	0.03 s
	11.284	[42]	13.71 ms	2.05 ms	3.80 ms	7.40 ms	1.27 ms
	11.494	[43]	4.21 ms	0.63 ms	1.20 ms	2.41 ms	0.40 ms
	8.966	[44]	11.10×10^{4} s	1.18×10^{4} s	1.77×10^{4} s	2.18×10^{4} s	0.60×10^{4} s
	10.764	[45]	30.09×10^{-2} s	6.19×10^{-2} s	10.98×10^{-2} s	13.72×10^{-2} s	2.58×10^{-2} s
^{288}118	13.365	[41]	29.68×10^{-7} s	3.97×10^{-7} s	8.42×10^{-7} s	12.05×10^{-7} s	2.71×10^{-7} s
	12.935	[42]	20.80 μs	2.84 μs	5.87 μs	7.93 μs	1.89 μs
	13.165	[43]	7.25 μs	0.98 μs	2.05 μs	2.86 μs	0.66 μs
	13.068	[44]	11.25 μs	1.53 μs	3.18 μs	4.38 μs	1.02 μs
	13.355	[45]	3.10 μs	0.54 μs	1.15 μs	1.26 μs	0.28 μs

TABLE II. (*Continued.*)

Nucleus	Q_α (MeV)		$T_{1/2}$ [37]	$T_{1/2}^{\mathrm{ERTR}}$ [39]	$T_{1/2}^{\mathrm{ERHR}}$ [39]	$T_{1/2}$ [30]	$T_{1/2}$ [34]
^{290}118	12.905	[41]	22.14 μs	3.00 μs	6.23 μs	9.07 μs	1.99 μs
	12.865	[42]	26.70 μs	3.63 μs	7.50 μs	10.87 μs	2.40 μs
	13.095	[43]	9.22 μs	1.24 μs	2.60 μs	3.89 μs	0.83 μs
	12.641	[44]	7.75×10^{-5} s	1.06×10^{-5} s	2.16×10^{-5} s	3.03×10^{-5} s	0.69×10^{-5} s
	12.455	[45]	19.25×10^{-5} s	3.57×10^{-5} s	7.15×10^{-5} s	7.27×10^{-5} s	1.71×10^{-5} s
^{292}118	12.535	[41]	5.76×10^{-5} s	1.63×10^{-5} s	3.33×10^{-5} s	4.98×10^{-5} s	1.06×10^{-5} s
	12.425	[42]	9.91×10^{-5} s	2.82×10^{-5} s	5.71×10^{-5} s	8.39×10^{-5} s	1.82×10^{-5} s
	12.645	[43]	3.38×10^{-5} s	0.96×10^{-5} s	1.96×10^{-5} s	2.98×10^{-5} s	0.62×10^{-5} s
	12.157	[44]	3.84×10^{-4} s	1.09×10^{-4} s	2.17×10^{-4} s	3.07×10^{-4} s	0.69×10^{-4} s
	12.205	[45]	3.00×10^{-4} s	1.17×10^{-4} s	2.31×10^{-4} s	2.43×10^{-4} s	0.54×10^{-4} s
^{294}118	12.175	[41]	62.19×10^{-5} s	9.17×10^{-5} s	18.38×10^{-5} s	28.14×10^{-5} s	5.82×10^{-5} s
	12.335	[42]	27.56×10^{-5} s	4.06×10^{-5} s	8.23×10^{-5} s	12.92×10^{-5} s	2.60×10^{-5} s
	12.565	[43]	8.82×10^{-5} s	1.30×10^{-5} s	2.67×10^{-5} s	4.33×10^{-5} s	0.84×10^{-5} s
	11.614	[44]	12.45 ms	1.81 ms	3.49 ms	4.89 ms	1.11 ms
	12.165	[45]	6.54×10^{-4} s	1.32×10^{-4} s	2.62×10^{-4} s	2.95×10^{-4} s	0.61×10^{-4} s
^{296}118	11.855	[41]	20.80×10^{-4} s	4.51×10^{-4} s	8.89×10^{-4} s	14.01×10^{-4} s	2.80×10^{-4} s
	12.345	[42]	16.30×10^{-5} s	3.55×10^{-5} s	7.25×10^{-5} s	12.31×10^{-5} s	2.28×10^{-5} s
	12.575	[43]	52.19 μs	11.33 μs	23.52 μs	41.30 μs	7.37 μs
	11.003	[44]	0.27 s	0.06 s	0.10 s	0.14 s	0.03 s
	12.125	[45]	5.01×10^{-4} s	1.49×10^{-4} s	2.98×10^{-4} s	3.60×10^{-4} s	0.69×10^{-4} s
^{298}118	11.555	[41]	26.60 ms	2.13 ms	4.13 ms	6.70 ms	1.29 ms
	12.565	[42]	13.05×10^{-5} s	1.09×10^{-5} s	2.28×10^{-5} s	4.33×10^{-5} s	0.71×10^{-5} s
	12.785	[43]	44.94 μs	3.77 μs	8.00 μs	15.63 μs	2.49 μs
	10.323	[44]	53.15 s	3.64 s	6.39 s	8.31 s	2.02 s
	12.035	[45]	19.40×10^{-4} s	2.19×10^{-4} s	4.39×10^{-4} s	5.63×10^{-4} s	1.00×10^{-4} s
^{300}118	11.295	[41]	69.35 ms	8.50 ms	16.30 ms	27.32 ms	5.07 ms
	12.775	[42]	28.64 μs	3.64 μs	7.76 μs	16.37 μs	2.40 μs
	12.995	[43]	10.20 μs	1.29 μs	2.79 μs	6.06 μs	0.86 μs
	9.567	[44]	6.77×10^{3} s	0.65×10^{3} s	1.07×10^{3} s	1.28×10^{3} s	0.34×10^{3} s
	12.045	[45]	10.98×10^{-4} s	1.91×10^{-4} s	3.86×10^{-4} s	5.36×10^{-4} s	0.88×10^{-4} s
^{302}118	11.055	[41]	0.24 s	0.03 s	0.06 s	0.10 s	0.02 s
	12.905	[42]	13.09 μs	1.81 μs	3.92 μs	9.07 μs	1.20 μs
	13.125	[43]	4.75 μs	0.65 μs	1.43 μs	3.41 μs	0.44 μs
	8.732	[44]	50.55×10^{5} s	4.36×10^{5} s	6.60×10^{5} s	7.04×10^{5} s	2.08×10^{5} s
	12.015	[45]	10.79×10^{-4} s	2.06×10^{-4} s	4.18×10^{-4} s	6.23×10^{-4} s	0.94×10^{-4} s
^{292}120	13.595	[41]	3.78 μs	0.48 μs	1.08 μs	1.49 μs	0.32 μs
	13.947	[42]	8.38×10^{-7} s	1.05×10^{-7} s	2.39×10^{-7} s	3.44×10^{-7} s	0.71×10^{-7} s
	14.187	[43]	31.11×10^{-8} s	3.81×10^{-8} s	8.84×10^{-8} s	13.09×10^{-8} s	2.63×10^{-8} s
	13.266	[44]	16.40 μs	2.13 μs	4.68 μs	6.15 μs	1.40 μs
	13.517	[45]	5.33 μs	0.92 μs	2.00 μs	2.07 μs	0.50 μs
^{294}120	13.195	[41]	9.66 μs	2.71 μs	5.97 μs	8.41 μs	1.77 μs
	13.357	[42]	4.63 μs	1.29 μs	2.87 μs	4.13 μs	0.85 μs
	13.587	[43]	1.67 μs	0.46 μs	1.04 μs	1.54 μs	0.31 μs
	12.746	[44]	8.04×10^{-5} s	2.29×10^{-5} s	4.90×10^{-5} s	6.48×10^{-5} s	1.46×10^{-5} s
	13.297	[45]	6.08 μs	2.25 μs	4.97 μs	5.37 μs	1.11 μs
^{296}120	12.825	[41]	9.54×10^{-5} s	1.43×10^{-5} s	3.10×10^{-5} s	4.49×10^{-5} s	0.92×10^{-5} s
	13.747	[42]	14.53×10^{-7} s	2.08×10^{-7} s	4.78×10^{-7} s	7.85×10^{-7} s	1.41×10^{-7} s
	13.977	[43]	5.50×10^{-7} s	0.78×10^{-7} s	1.80×10^{-7} s	3.05×10^{-7} s	0.53×10^{-7} s
	12.170	[44]	2.56 ms	0.39 ms	0.80 ms	1.05 ms	0.24 ms
	13.287	[45]	11.05 μs	2.16 μs	4.81 μs	5.61 μs	1.07 μs
^{298}120	12.485	[41]	30.24×10^{-5} s	7.03×10^{-5} s	14.99×10^{-5} s	22.34×10^{-5} s	4.40×10^{-5} s
	13.417	[42]	3.65 μs	0.83 μs	1.87 μs	3.18 μs	0.55 μs
	13.637	[43]	1.38 μs	0.31 μs	0.71 μs	1.24 μs	0.21 μs
	11.534	[44]	4.99×10^{-5} s	1.13×10^{-5} s	2.24×10^{-5} s	2.88×10^{-5} s	0.66×10^{-5} s
	13.507	[45]	2.45 μs	0.73 μs	1.66 μs	2.16 μs	0.37 μs
^{300}120	12.165	[41]	15.44×10^{-4} s	3.34×10^{-4} s	7.01×10^{-4} s	10.74×10^{-4} s	2.04×10^{-4} s
	13.457	[42]	3.01 μs	0.64 μs	1.45 μs	2.68 μs	0.42 μs

TABLE II. (*Continued.*)

Nucleus	Q_α (MeV)		$T_{1/2}$ [37]	$T_{1/2}^{\mathrm{ERTR}}$ [39]	$T_{1/2}^{\mathrm{ERHR}}$ [39]	$T_{1/2}$ [30]	$T_{1/2}$ [34]
	13.687	[43]	1.10 μs	0.23 μs	0.53 μs	1.01 μs	0.15 μs
	10.842	[44]	3.17 s	0.63 s	1.19 s	1.46 s	0.35 s
	13.177	[45]	10.69 μs	3.04 μs	6.82 μs	9.12 μs	1.49 μs
^{302}120	11.875	[41]	12.39 ms	1.44 ms	2.98 ms	4.71 ms	0.86 ms
	13.777	[42]	12.37×10^{-7} s	1.42×10^{-7} s	3.34×10^{-7} s	6.93×10^{-7} s	0.96×10^{-7} s
	14.007	[43]	4.68×10^{-7} s	0.53×10^{-7} s	1.26×10^{-7} s	2.70×10^{-7} s	0.36×10^{-7} s
	10.092	[44]	8.42×10^{2} s	0.79×10^{2} s	1.42×10^{2} s	1.62×10^{2} s	0.42×10^{2} s
	13.137	[45]	21.47 μs	3.37 μs	7.60 μs	10.90 μs	1.65 μs
^{304}120	11.605	[41]	46.60 ms	5.87 ms	11.99 ms	19.58 ms	3.46 ms
	13.887	[42]	6.57×10^{-7} s	0.81×10^{-7} s	1.93×10^{-7} s	4.40×10^{-7} s	0.55×10^{-7} s
	14.117	[43]	25.21×10^{-8} s	3.06×10^{-8} s	7.40×10^{-8} s	17.31×10^{-8} s	2.11×10^{-8} s
	9.290	[44]	30.54×10^{4} s	2.69×10^{4} s	4.45×10^{4} s	4.62×10^{4} s	1.31×10^{4} s
	13.127	[45]	18.96 μs	3.25 μs	7.37 μs	11.39 μs	1.59 μs
^{306}120	12.515	[41]	33.84×10^{-5} s	4.32×10^{-5} s	9.51×10^{-5} s	19.32×10^{-5} s	2.71×10^{-5} s
	14.327	[42]	10.09×10^{-8} s	1.18×10^{-8} s	2.91×10^{-8} s	7.54×10^{-8} s	0.82×10^{-8} s
	14.567	[43]	39.14 ns	4.48 ns	11.18 ns	29.79 ns	3.16 ns
	13.787	[45]	9.41×10^{-7} s	1.51×10^{-7} s	3.58×10^{-7} s	6.65×10^{-7} s	0.78×10^{-7} s
^{296}122	13.885	[41]	14.95×10^{-7} s	4.49×10^{-7} s	10.68×10^{-7} s	14.14×10^{-7} s	2.95×10^{-7} s
	14.568	[42]	8.98×10^{-8} s	2.54×10^{-8} s	6.28×10^{-8} s	9.05×10^{-8} s	1.73×10^{-8} s
	14.798	[43]	3.66×10^{-8} s	1.01×10^{-8} s	2.53×10^{-8} s	3.74×10^{-8} s	0.70×10^{-8} s
	13.225	[44]	28.46 μs	8.89 μs	20.27 μs	24.57 μs	5.63 μs
^{298}122	13.495	[41]	16.95 μs	2.34 μs	5.48 μs	7.46 μs	1.51 μs
	14.978	[42]	37.17 ns	4.57 ns	11.63 ns	19.03 ns	3.18 ns
	15.218	[43]	15.19 ns	1.81 ns	4.68 ns	7.87 ns	1.28 ns
	12.616	[44]	11.18×10^{-4} s	1.57×10^{-4} s	3.47×10^{-4} s	4.17×10^{-4} s	0.96×10^{-4} s
^{300}122	13.125	[41]	5.21×10^{-5} s	1.20×10^{-5} s	2.76×10^{-5} s	3.86×10^{-5} s	0.76×10^{-5} s
	14.048	[42]	8.48×10^{-7} s	1.87×10^{-7} s	4.56×10^{-7} s	7.21×10^{-7} s	1.24×10^{-7} s
	14.288	[43]	31.27×10^{-8} s	6.78×10^{-8} s	16.74×10^{-8} s	27.27×10^{-8} s	4.56×10^{-8} s
	11.962	[44]	19.56 ms	4.45 ms	9.44 ms	10.08 ms	2.60 ms
^{302}122	12.775	[41]	29.78×10^{-5} s	6.01×10^{-5} s	13.61×10^{-5} s	19.56×10^{-5} s	3.71×10^{-5} s
	14.108	[42]	6.92×10^{-7} s	1.33×10^{-7} s	3.28×10^{-7} s	5.64×10^{-7} s	0.89×10^{-7} s
	14.358	[43]	2.47×10^{-7} s	0.47×10^{-7} s	1.16×10^{-7} s	2.06×10^{-7} s	0.31×10^{-7} s
	11.269	[44]	1.13 s	0.21 s	0.43 s	0.49 s	0.12 s
^{304}122	12.455	[41]	32.12×10^{-4} s	2.77×10^{-4} s	6.18×10^{-4} s	9.15×10^{-4} s	1.67×10^{-4} s
	14.878	[42]	64.85 ns	5.23 ns	13.55 ns	27.67 ns	3.63 ns
	15.118	[43]	26.09 ns	2.06 ns	5.40 ns	11.34 ns	1.44 ns
	10.543	[44]	262.23 s	18.56 s	35.54 s	37.87 s	9.73 s
^{306}122	12.165	[41]	12.36 ms	1.16 ms	2.55 ms	3.90 ms	0.69 ms
	14.988	[42]	36.25 ns	3.13 ns	8.21 ns	18.33 ns	2.18 ns
	15.218	[43]	15.33 ns	1.29 ns	3.43 ns	7.87 ns	0.91 ns
	9.794	[44]	46.41×10^{3} s	3.15×10^{3} s	5.65×10^{3} s	5.57×10^{3} s	1.54×10^{3} s
^{308}122	13.805	[41]	3.32 μs	0.38 μs	0.95 μs	1.98 μs	0.2.5 μs
	15.508	[42]	4.06 ns	0.40 ns	1.09 ns	2.78 ns	0.29 ns
	15.748	[43]	17.44×10^{-10} s	1.67×10^{-10} s	4.59×10^{-10} s	12.02×10^{-10} s	1.21×10^{-10} s
^{310}122	13.465	[41]	14.03 μs	1.62 μs	3.95 μs	8.50 μs	1.04 μs
	15.168	[42]	13.10 ns	1.32 ns	3.56 ns	9.44 ns	0.93 ns
	15.408	[43]	5.45 ns	0.54 ns	1.46 ns	3.97 ns	0.38 ns
^{300}124	14.175	[41]	15.25×10^{-7} s	4.19×10^{-7} s	10.57×10^{-7} s	13.43×10^{-7} s	2.71×10^{-7} s
	15.690	[42]	4.31 ns	1.01 ns	2.76 ns	4.19 ns	0.70 ns
	15.940	[43]	1.79 ns	0.40 ns	1.12 ns	1.75 ns	0.30 ns
	12.939	[44]	4.27×10^{-4} s	1.24×10^{-4} s	2.89×10^{-4} s	3.10×10^{-4} s	0.75×10^{-4} s
^{302}124	13.785	[41]	10.04 μs	2.13 μs	5.29 μs	6.91 μs	1.35 μs
	13.950	[42]	4.86 μs	1.02 μs	2.57 μs	3.43 μs	0.66 μs
	14.200	[43]	16.64×10^{-7} s	3.46×10^{-7} s	8.79×10^{-7} s	12.12×10^{-7} s	2.24×10^{-7} s
	12.280	[44]	15.65 ms	3.33 ms	7.46 ms	7.85 ms	1.92 ms
^{304}124	13.405	[41]	17.23×10^{-5} s	1.11×10^{-5} s	2.72×10^{-5} s	3.65×10^{-5} s	0.69×10^{-5} s
	13.700	[42]	44.41 μs	2.87 μs	7.13 μs	9.96 μs	1.81 μs

TABLE II. (*Continued.*)

Nucleus	Q_α (MeV)		$T_{1/2}$ [37]	$T_{1/2}^{\mathrm{ERTR}}$ [39]	$T_{1/2}^{\mathrm{ERHR}}$ [39]	$T_{1/2}$ [30]	$T_{1/2}$ [34]
	13.950	[43]	14.61 μs	0.94 μs	2.37 μs	3.43 μs	0.60 μs
	11.605	[44]	22.43×10^{-1} s	1.30×10^{-1} s	2.80×10^{-1} s	2.85×10^{-1} s	0.72×10^{-1} s
$^{306}124$	13.055	[41]	2.33×10^{-5} s	5.43×10^{-5} s	13.05×10^{-5} s	18.00×10^{-5} s	3.30×10^{-5} s
	16.390	[42]	8.15×10^{-11} s	6.40×10^{-11} s	18.53×10^{-11} s	38.29×10^{-11} s	4.62×10^{-11} s
	16.630	[43]	3.95×10^{-11} s	2.82×10^{-11} s	8.25×10^{-11} s	17.46×10^{-11} s	2.05×10^{-11} s
	10.927	[44]	2.11s	7.34 s	15.00 s	14.59 s	3.84 s
$^{308}124$	12.725	[41]	29.14×10^{-4} s	2.56×10^{-4} s	6.06×10^{-4} s	8.61×10^{-4} s	1.52×10^{-4} s
	16.200	[42]	15.83×10^{-10} s	1.14×10^{-10} s	3.30×10^{-10} s	7.22×10^{-10} s	0.82×10^{-10} s
	16.450	[43]	6.87×10^{-10} s	0.48×10^{-10} s	1.40×10^{-10} s	3.14×10^{-10} s	0.35×10^{-10} s
	10.268	[44]	81.82×10^{2} s	5.41×10^{2} s	10.49×10^{2} s	9.68×10^{2} s	2.68×10^{2} s
$^{310}124$	15.145	[41]	52.39 ns	5.20 ns	14.36 ns	30.20 ns	3.54 ns
	16.390	[42]	63.79×10^{-11} s	5.41×10^{-11} s	15.90×10^{-11} s	38.29×10^{-11} s	3.90×10^{-11} s
	16.640	[43]	28.22×10^{-11} s	2.30×10^{-11} s	6.85×10^{-11} s	16.91×10^{-11} s	1.68×10^{-11} s
$^{312}124$	14.845	[41]	18.71×10^{-8} s	1.57×10^{-8} s	4.28×10^{-8} s	9.39×10^{-8} s	1.05×10^{-8} s
	15.360	[42]	26.34 ns	2.09 ns	5.88 ns	13.68 ns	1.44 ns
	15.600	[43]	10.91 ns	0.85 ns	2.41 ns	5.76 ns	0.59 ns
$^{314}124$	14.495	[41]	6.57×10^{-7} s	0.60×10^{-7} s	1.63×10^{-7} s	3.68×10^{-7} s	0.40×10^{-7} s
	14.310	[42]	14.10×10^{-7} s	1.31×10^{-7} s	3.49×10^{-7} s	7.74×10^{-7} s	0.85×10^{-7} s
	14.550	[43]	5.25×10^{-7} s	0.48×10^{-7} s	1.30×10^{-7} s	2.96×10^{-7} s	0.32×10^{-7} s
$^{304}126$	14.455	[41]	3.81 μs	0.41 μs	1.09 μs	1.33 μs	0.26 μs
	12.475	[44]	44.56 ms	4.82 ms	11.32 ms	10.42 ms	2.73 ms
$^{306}126$	14.045	[41]	1.34 μs	2.22 μs	5.83 μs	7.26 μs	1.38 μs
	13.752	[42]	4.63 μs	8.30 μs	21.39 μs	25.62 μs	5.08 μs
	14.002	[43]	1.60 μs	2.69 μs	7.04 μs	8.71 μs	1.67 μs
	11.8460	[44]	5.28×10^{-2} s	14.08×10^{-2} s	31.74×10^{-2} s	28.51×10^{-2} s	7.62×10^{-2} s
$^{308}126$	13.665	[41]	6.14 μs	11.37 μs	29.36 μs	37.55 μs	6.92 μs
	19.381	[42]	8.60×10^{-14} s	1.89×10^{-14} s	6.43×10^{-14} s	14.95×10^{-14} s	1.49×10^{-14} s
	19.642	[43]	48.01 fs	9.32 fs	32.06 fs	76.12 fs	7.40 fs
	11.257	[44]	1.45 s	4.28 s	9.26 s	8.10 s	2.21 s
$^{310}126$	13.305	[41]	6.93×10^{-4} s	0.57×10^{-4} s	1.45×10^{-4} s	1.90×10^{-4} s	0.34×10^{-4} s
	17.071	[42]	28.90×10^{-11} s	1.79×10^{-11} s	5.57×10^{-11} s	11.40×10^{-11} s	1.29×10^{-11} s
	17.322	[43]	13.24×10^{-11} s	0.77×10^{-11} s	2.48×10^{-11} s	5.20×10^{-11} s	0.57×10^{-11} s
	10.737	[44]	17.04×10^{2} s	1.09×10^{2} s	2.28×10^{2} s	1.95×10^{2} s	0.54×10^{2} s
$^{312}126$	14.815	[41]	6.42×10^{-7} s	0.65×10^{-7} s	1.83×10^{-7} s	3.16×10^{-7} s	0.42×10^{-7} s
	16.592	[42]	9.92×10^{-10} s	0.83×10^{-10} s	2.54×10^{-10} s	5.36×10^{-10} s	0.58×10^{-10} s
	16.842	[43]	4.39×10^{-10} s	0.35×10^{-10} s	1.10×10^{-10} s	2.37×10^{-10} s	0.25×10^{-10} s
$^{314}126$	12.935	[41]	32.25×10^{-4} s	2.95×10^{-4} s	7.43×10^{-4} s	10.78×10^{-4} s	1.72×10^{-4} s
	15.752	[42]	19.26 ns	1.55 ns	4.60 ns	9.56 ns	1.05 ns
	16.011	[43]	7.65 ns	0.60 ns	1.79 ns	3.84 ns	0.41 ns
$^{316}126$	11.295	[41]	28.92 s	2.41 s	5.40 s	6.46 s	1.25 s
	15.101	[42]	19.91×10^{-8} s	1.74×10^{-8} s	5.04×10^{-8} s	10.50×10^{-8} s	1.15×10^{-8} s
	15.352	[43]	76.11 ns	6.51 ns	19.09 ns	40.92 ns	4.34 ns
$^{318}126$	9.965	[41]	25.77×10^{4} s	1.74×10^{4} s	3.47×10^{4} s	3.43×10^{4} s	0.81×10^{4} s
	14.521	[42]	18.37×10^{-7} s	1.72×10^{-7} s	4.85×10^{-7} s	10.16×10^{-7} s	1.10×10^{-7} s
	14.771	[43]	6.61×10^{-7} s	0.61×10^{-7} s	1.74×10^{-7} s	3.76×10^{-7} s	0.39×10^{-7} s

are very illustrative and useful. Comparing results in Table II and Fig. 1 we can conclude the following.

(i) The difference between values of α-decay half-lives induced by applying various approaches for half-life evaluation is smaller then 20 times for the SHE region.

(ii) Various approaches for atomic masses predict very different values and mass dependence of Q values in the region $Z = 118$–126. The difference between Q values evaluated using various approaches for atomic masses increases with Z. This difference between Q values is very dramatic for $Z = 126$ and $N = 184$, where it reaches approximately 8.4 MeV.

(iii) Very different values of α-decay half-lives of SHEs can be obtained by applying various approximations for atomic masses. Then, using the same approximation for the evaluation of α-decay half-life and different atomic mass models for the Q value of α transition, the evaluated values of half-lives can vary in 15 orders (see results for SHEs with $Z = 126$).

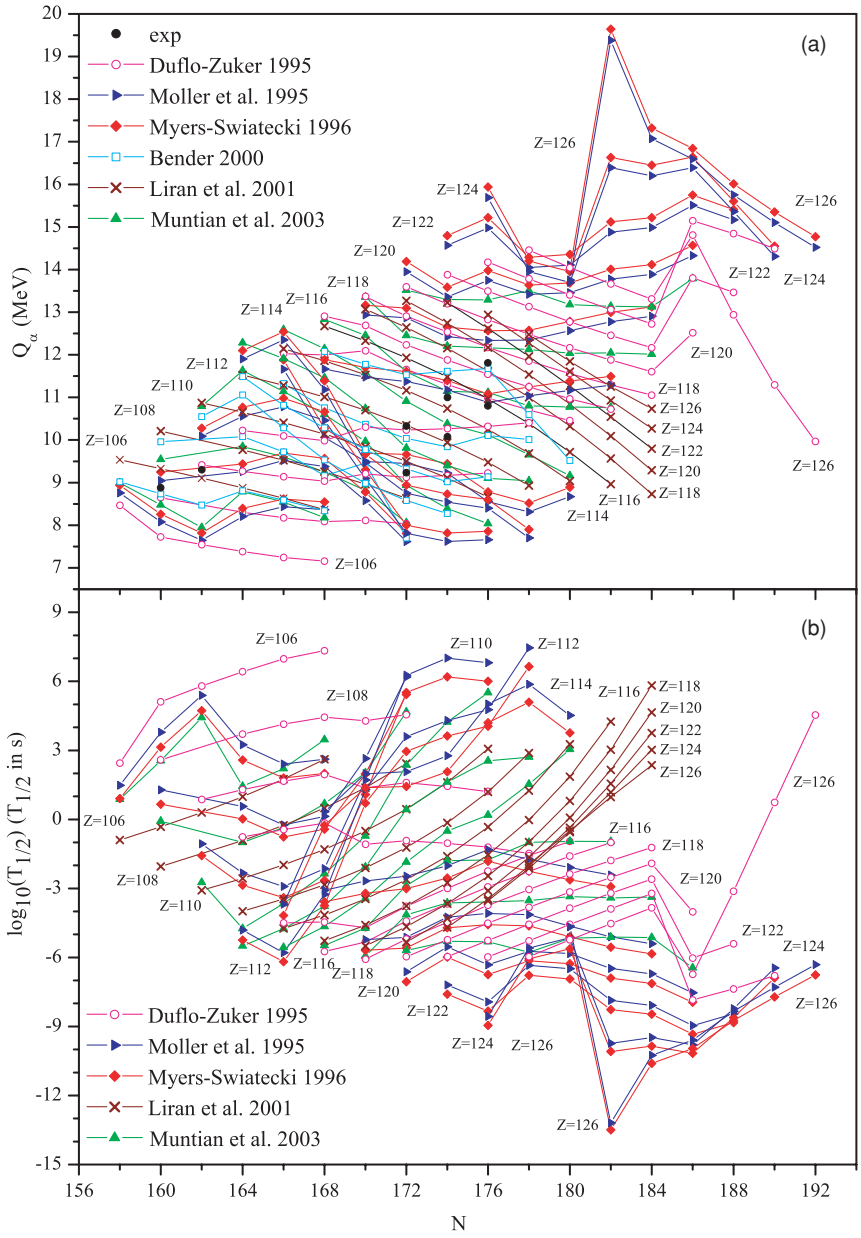

FIG. 1. (Color online) (a) The Q values of α transitions between the ground states of nuclei as a function of the neutron number (N) calculated in the framework of the different approaches [41–46]. The Q values are evaluated by Duflo and Zuker [41], Möller *et al.* [42], Myers and Swiatecki [43], Bender [46], Liran *et al.* [44], and Muntian *et al.* [45]. The available experimental values are marked by solid circles. (b) $\log_{10}T_{1/2}$ as a function of the neutron number (N) evaluated in the framework of the ERHR by using different approaches for the Q values [41–45].

(iv) Experimental studies of SHEs with $Z = 126$ and $N = 184$ and others like them are extremely important because strong variation of α-decay half-life values for this SHE induced by different atomic mass models can be used for the discrimination of successful theoretical approaches for atomic masses. Note that this is very important from the aspect of a magic proton number for the SHE region.

Note that different nuclear models predict different values of both the atomic masses and the magic numbers for the SHE region. The predictions, in the framework of the different approaches [22,50,51] (and see references cited therein), more often name $Z = 114, 120, 124, 126, 164$ and $N = 164, 172, 184, 228, 258$ as magic numbers. Therefore, experimental studies of SHEs with $Z = 126$ and $N = 184$ can help greatly in the further development of theory.

Similar approaches for atomic masses [20,42,43,45] based on extended Weizsäcker formula and the Strutinsky shell corrections [19] lead to similar Q values of α transitions. However, the differences between Q values evaluated in the framework of these approaches increase with Z and reach maximal values for $Z = 126$. The magic numbers for these approaches are $Z = 114$ and $N = 184$. However, note that the magic numbers for the SHE region depend on the mean-field parametrizations [22,50]. The Q values obtained in these approaches are largest for the range $120 \leqslant Z \leqslant 126$; therefore, the α-decay half-lives of even-even SHEs are smallest in comparison with other approaches. The Q values obtained by using prediction of the mass formula of Liran *et al.* [44] are very different from others for $Z \geqslant 118$ and lead to the longest α-decay half-lives of SHEs. The magic numbers $Z = 126$ and $N = 184$ are proposed by Liran *et al.* [44]. The Q values calculated with the help of the Duflo and Zuker mass

formula [41] are between the ones obtained in the framework of [42,43,45] and [44] mass models for $Z \geqslant 120$; therefore, α-decay half-lives occupy intermediate values between these two different approaches.

The atomic masses are tabulated in Refs. [20,45] in the range $\leqslant$120. Therefore, α-decay Q values and corresponding half-lives can be also calculated in the range $Z \leqslant 120$. However, we suppose that the behavior of α-decay Q values and corresponding half-lives for $Z > 120$ evaluated by using atomic masses [20,45] will be similar to the ones presented in Fig. 1 and Table II for similar approaches for atomic masses [42,43].

In conclusion, we have estimated the α-decay half-lives of even-even SHEs within the range of proton numbers $104 \leqslant Z \leqslant 126$, which may be formed by possible cold and hot fusion reactions, in the framework of various approaches for α-decay half-life evaluation and by using the Q values of α transitions obtained within different approximations for atomic masses. Spectacular differences between the Q values and half-lives calculated in the framework of various approaches in the range $Z \geqslant 118$ and $180 \leqslant N \leqslant 192$ can be used for discrimination of a correct theoretical approach for atomic masses. Because of this, experimental studies of SHEs with $Z = 126$ and $N = 184$ are very desirable.

ACKNOWLEDGMENTS

We are grateful to Andres Zuker for the code of mass formulas [41] and comments on it.

[1] S. Hofmann and G. Münzenberg, Rev. Mod. Phys. **72**, 733 (2000); Yu. Ts. Oganessian, Nucl. Phys. A **834**, 331c (2010).
[2] Ch. Stodel *et al.*, AIP Conf. Proc. **891**, 55 (2007).
[3] S. Hofmann *et al.*, Eur. Phys. J. A **10**, 5 (2001).
[4] S. Hofmann, Eur. Phys. J. A **15**, 195 (2002).
[5] S. Hofmann *et al.*, J. Nucl. Radiochem. Sci. **7**, R25 (2006).
[6] S. Hofmann *et al.*, Eur. Phys. J. A **32**, 251 (2007).
[7] S. Hofmann, Prog. Part. Nucl. Phys. **62**, 337 (2009).
[8] Z. G. Gan *et al.*, Eur. Phys. J. A **20**, 385 (2004).
[9] H. Ikezoe *et al.*, Eur. Phys. J. A **2**, 379 (1998).
[10] Yu. Ts. Oganessian *et al.*, Phys. Rev. C **74**, 044602 (2006).
[11] Yu. Ts. Oganessian, Phys. At. Nucl. **69**, 932 (2006); J. Phys. G **34**, R165 (2007).
[12] Yu. Ts. Oganessian *et al.*, Nucl. Phys. A **682**, 108c (2001).
[13] L. Stavsetra, K. E. Gregorich, J. Dvorak, P. A. Ellison, I. Dragojevic, M. A. Garcia, and H. Nitsche, Phys. Rev. Lett. **103**, 132502 (2009).
[14] K. Morita *et al.*, J. Phys. Soc. Jpn. **73**, 2593 (2004).
[15] S. Ketelhut *et al.*, Phys. Rev. Lett. **102**, 212501 (2009).
[16] R.-D. Herzberg and P. T. Greenlees, Prog. Part. Nucl. Phys. **61**, 674 (2008).
[17] V. Yu. Denisov and S. Hofmann, Phys. Rev. C **61**, 034606 (2000).
[18] V. Yu. Denisov and W. Nörenberg, Eur. Phys. J. A **15**, 375 (2002); V. Yu. Denisov and N. A. Pilipenko, Phys. Rev. C **76**, 014602 (2007).
[19] V. M. Strutinsky, Nucl. Phys. A **95**, 420 (1967); **122**, 1 (1968); M. Brack *et al.*, Rev. Mod. Phys. **44**, 320 (1972).
[20] R. Smolańczuk, J. Skalski, and A. Sobiczewski, Phys. Rev. C **52**, 1871 (1995); R. Smolańczuk, *ibid.* **56**, 812 (1997); A. Sobiczewski and I. Muntian, Nucl. Phys. A **734**, 176 (2004); I. Muntian, Z. Patyk, and A. Sobiczewski, Acta Phys. Pol. B **34**, 2141 (2003).
[21] J. F. Berger, D. Hirata, and M. Girod, Acta Phys. Pol. B **34**, 1909 (2003).
[22] V. Yu. Denisov, Phys. At. Nucl. **68**, 1133 (2005).
[23] A. Sobiczewski and K. Pomorski, Prog. Part. Nucl. Phys. **58**, 292 (2007); A. Sobiczewski, Acta Phys. Pol. B **41**, 157 (2010).
[24] P. Möller, A. J. Sierk, T. Ichikawa, A. Iwamoto, R. Bengtsson, H. Uhrenholt, and S. Aberg, Phys. Rev. C **79**, 064304 (2009).
[25] J. C. Pei, W. Nazarewicz, J. A. Sheikh, and A. K. Kerman, Phys. Rev. Lett. **102**, 192501 (2009).
[26] S. B. Duarte *et al.*, At. Data Nucl. Data Tables **80**, 235 (2002).
[27] V. Yu Denisov and H. Ikezoe, Phys. Rev. C **72**, 064613 (2005).
[28] M. Gupta and T. W. Burrows, Nucl. Data Sheets **106**, 251 (2005).
[29] C. Xu and Z. Ren, Nucl. Phys. A **753**, 174 (2005).
[30] A. Sobiczewski and A. Parkhomenko, Phys. At. Nucl. **69**, 1155 (2006).
[31] D. N. Poenaru, I.-H. Plonski, and W. Greiner, Phys. Rev. C **74**, 014312 (2006).
[32] I. Silisteanu, A. Neacsu, A. O. Silisteanu, and M. Rizea, AIP Conf. Proc. **972**, 505 (2008).
[33] P. R. Chowdhury, C. Samanta, and D. N. Basu, At. Data Nucl. Data Tables **94**, 781 (2008).
[34] G. Royer and H. F. Zhang, Phys. Rev. C **77**, 037602 (2008).
[35] K. P. Santhosh, S. Sahadevan, and R. K. Biju, Nucl. Phys. A **825**, 159 (2009).
[36] N. Dasgupta-Schubert, M. A. Reyes, and V. A. Tamez, Eur. Phys. J. A **42**, 121 (2009).
[37] V. Yu. Denisov and A. A. Khudenko, At. Data Nucl. Data Tables **95**, 815 (2009).
[38] V. Yu. Denisov and A. A. Khudenko, Phys. Rev. C **80**, 034603 (2009).
[39] V. Yu. Denisov and A. A. Khudenko, Phys. Rev. C **79**, 054614 (2009).
[40] G. Audi, O. Bersillon, J. Blachot, and A. H. Wapstra, Nucl. Phys. A **729**, 3 (2003).
[41] J. Duflo and A. P. Zuker, Phys. Rev. C **52**, R23 (1995).
[42] P. Möller, J. R. Nix, W. D. Myers, and W. J. Swiatecki, At. Data Nucl. Data Tables **59**, 185 (1995).
[43] W. D. Myers and W. J. Swiatecki, Nucl. Phys. A **601**, 141 (1996).
[44] S. Liran, A. Marinov, and N. Zeldes, arXiv:nucl-th/0102055; Phys. Rev. C **66**, 024303 (2002).
[45] I. Muntian, Z. Patyk, and A. Sobiczewski, Acta Phys. Pol. B **32**, 691 (2001); Phys. At. Nucl. **66**, 1015 (2003); I. Muntian, S. Hofmann, Z. Patyk, and A. Sobiczewski, Acta Phys. Pol. B **34**, 2073 (2003).
[46] M. Bender, Phys. Rev. C **61**, 031302(R) (2000).
[47] J. O. Rasmussen, in *Alpha-, Beta-, and Gamma-ray Spectroscopy*, edited by K. Siegbahn (North–Holland, Amsterdam, 1965), Vol. I.
[48] P. Möller, J. R. Nix, and K.-L. Kratz, At. Data Nucl. Data Tables **66**, 131 (1995).
[49] E. L. Medeiros, M. M. N. Rodrigues, S. B. Duarte, and O. A. P. Tavares, J. Phys. G **32**, B23 (2006).
[50] V. Yu. Denisov, Phys. At. Nucl. **70**, 244 (2007).
[51] M. Bender, P.-H. Heenen, and P.-G. Reinhard, Rev. Mod. Phys. **75**, 121 (2003).